

# *HST* Imaging of the Host Galaxies of Three X-Ray Selected BL Lacertae Objects<sup>1</sup>

Buell T. Jannuzi

National Optical Astronomy Observatories, P.O. Box 26732, Tucson, AZ 85726-6732, USA

Email: [bjannuzi@noao.edu](mailto:bjannuzi@noao.edu)

Brian Yanny

Fermi National Accelerator Lab., Batavia, IL 60510, USA

Email: [yanny@sdss.fnal.gov](mailto:yanny@sdss.fnal.gov)

Chris Impey

Steward Observatory, University of Arizona, Tucson, AZ 85721, USA

Email: [impey@as.arizona.edu](mailto:impey@as.arizona.edu)

## ABSTRACT

*Hubble Space Telescope* (*HST*) WFPC-2 *I*-band (F814W) images of three X-ray selected BL Lacertae objects (MS 1221.8+2452, MS 1407.9+5954, & MS 2143.4+0704) reveal that each of these BL Lac objects is well-centered in an extended nebulosity that is consistent in brightness and morphology with being light from an elliptical galaxy at the previously reported redshifts of these BL Lac objects. Each of the detected host galaxies have radial surface brightness profiles that are well fit by a De Vaucouleurs law with effective radii of between 3 to 12 kpc ( $H_0 = 50 \text{ km s}^{-1} \text{ Mpc}^{-1}$ ,  $q_0 = 0$ ). The absolute magnitudes of the host galaxies fall in the range  $-24.7 < M_I < -23.5$ , in the range of luminosities determined for other BL Lacertae object host galaxies.

In addition to allowing the measurement of the host galaxy magnitudes and radial surface brightness profiles, the *HST* images allow a search for substructure in the host galaxies and the presence of close companion galaxies at spatial resolutions not yet achievable from the ground. While no evidence was found for any “bars” or spiral arms, “boxy” isophotes are present in the host galaxy of at least one of the three objects observed as part of this study (MS 2143.4+0704). The apparent magnitudes and image properties of the companions of the BL Lac

---

<sup>1</sup>Based on observations with the NASA/ESA *Hubble Space Telescope*, obtained at the Space Telescope Science Institute, which is operated by the Association of Universities for Research in Astronomy, Inc., under NASA contract NAS5-26555.

objects are catalogued as part of this work. The three BL Lacs appear to occur in diverse environments, from being fairly isolated (MS 1221.8+2452) to possibly being a member of a rich group of galaxies (MS 1407.9+5954).

*Subject headings:* BL Lac objects: individual (MS 1221.8+2452, MS 1407.9+5954, MS 2143.4+0704) – galaxies: active – galaxies: photometry

To appear in *The Astrophysical Journal Nov 20, 1997*

## 1. Introduction

The spectral energy distributions of catalogued BL Lacertae objects are dominated from radio to ultraviolet wavelengths by the variable and polarized emission of a compact synchrotron source (*e.g.* Impey and Neugebauer 1988; Wagner & Witzel 1995). The synchrotron emission is believed to be generated in a “jet” of relativistic material viewed nearly along the jet axis (Blandford & Rees 1978). The Doppler boosting of the emission to large apparent luminosities results in a very bright point source at optical and IR wavelengths and greatly complicates efforts to observe the nearby environment of BL Lac objects.

Observations of the surrounding nebulosities (or host galaxies) and companions of BL Lacertae objects are of particular interest because they provide direct tests of proposed unification schemes between BL Lac objects and other classes of AGNs or radio galaxies (*e.g.* with Farnaroff-Riley I radio galaxies, Urry & Padovani 1995) and allow the investigation of the role of the nearby environment in generating and maintaining the observed properties of BL Lacertae objects. Despite the difficulties caused by the bright point sources of BL Lacs, studies of the host galaxies of BL Lacs have been successfully undertaken from the ground for over 20 years (Oke & Gunn 1974; Thuan, Oke, & Gunn 1975; Ulrich *et al.* 1975; Miller, French, & Hawley 1978; and many others including: Ulrich 1989; Abraham *et al.* 1991; Pesce, Falomo, & Treves 1994, 1995; Wurtz, Stocke, & Yee 1996, hereafter WSY; Wurtz *et al.* 1997; Falomo 1996, and references therein). While we will review some of these past results in §3.2, the main result of the past work can be generalized as follows: whenever the host galaxies of BL Lacs have been well observed they have proven to be elliptical galaxies.

Despite the impressive past results, the majority of well observed host galaxies are at low redshift ( $z < 0.6$ ) or of BL Lacs that do not have large ratios of observed nuclear

brightness to surrounding nebulosity. Studies of BL Lacs using the high spatial resolution obtainable with the *Hubble Space Telescope* (*HST*) have now been made, with advantages over ground based observations for measuring the properties of the host galaxy close to the nucleus (a factor of 2 to 10 times closer depending on the quality of the ground-based imaging) and for detecting close companions (Falomo *et al.* 1997; Yanny, Jannuzi, & Impey 1997).

Unfortunately, the number of BL Lacs that have been well imaged with *HST* is small and well behind the significant number of luminous quasars that have been observed (*e.g.* Disney *et al.* 1995; McLeod & Rieke 1995; Bahcall *et al.* 1997, and references therein; Hooper, Impey, & Foltz 1997). Efforts to obtain a significant sample of well *HST* imaged BL Lacs are in progress by two groups of researchers, a team led by C. M. Urry and our team. We coordinated target selection and filter and detector choices in an attempt to provide, in the end, as large and homogeneous a data set as possible. The WFPC-2 PC was chosen as the instrument to use because of its large dynamic range and pixel scale. The F814W filter is used in these BL Lac host observations to allow comparison with ground based  $I_{\text{KC}}$ -band fluxes and to maximize the contrast of a host galaxy (expected to be red in color) over the non-thermal point source.

First results from the Urry team on the imaging of three radio selected BL Lacs are presented by Falomo *et al.* (1997). Two of these objects were found to be in luminous elliptical hosts, while no underlying host was detected for the third. We have previously reported results of our imaging of the radio selected BL Lac object OJ 287 (Yanny *et al.* 1997), which might have an off-centered host galaxy or show evidence of a recent interaction with a close companion galaxy. In this paper we present (*HST*) WFPC-2 images of three X-ray selected BL Lacertae objects (XSBLs), MS 1221.8+2452, MS 1407.9+5954, and MS 2143.4+0704, and discuss what can be learned about their host galaxies and surrounding environment. To ease comparison to the analysis of *HST* imaging of BL Lacs published by Falomo *et al.* (1997), we adopt the same cosmological parameters ( $H_0 = 50$  km s<sup>-1</sup> Mpc<sup>-1</sup>,  $q_0 = 0$ ) when deriving absolute luminosities and other physical properties of the host galaxies.

## 2. Observations

### 2.1. Sample Definition

We selected the three objects discussed in this paper for observation with *HST* because they are all X-ray selected BL Lac objects in the complete flux limited *Einstein* Observatory

Extended Medium Sensitivity Survey (*EMSS*) sample of BL Lac objects (Morris *et al.* 1991). While not evident from the study of individual objects, some differences in the typical properties of BL Lacs selected at different wavelength bands (*e.g.* X-ray and radio) have been noted, particularly in the degree of variability in the total and polarized optical flux and the polarization position angle (see Stocke *et al.* 1985, WSY, Jannuzi 1990, and Jannuzi, Smith, & Elston 1993, 1994 for examples of further discussion). Ultimately, if a larger database of observations can be compiled, we hope to be able to compare the more isotropic properties of various BL Lac subsamples (host galaxy properties, group and cluster environments, etc.). Some such comparisons have been made by WSY from their CFHT imaging survey of 50 objects. Finding charts and coordinates for the three fields whose images are presented in this paper may be found in Smith, Jannuzi & Elston (1991).

## 2.2. WFPC-2 Imaging

Our observations consisted of multiple long and short exposures with the WFPC-2 camera of the *HST* in the F814W filter. For references on the WFPC-2 instrument, see *e.g.* Holtzman *et al.* (1995). For MS 1221.8+2452, three 500s and two 200s exposures were obtained on 1996 January 13 UT. For MS 1407.9+5954, four 900s and three 160s exposures were taken on 1995 October 22 UT, and for MS 2143.4+0704, two 1100s and five 350s exposures were recorded on 1995 September 8 UT. The short exposures were designed to ensure at least some images of each BL Lac were obtained without saturated cores. In practice, none of the three variable BL Lac nuclei were bright enough at the time it was imaged to saturate the detector during even the longest exposures we obtained. Therefore all exposures of an object were simply averaged together, weighted by exposure time and with cosmic ray rejection (Yanny *et al.* 1994).

For each of the three BL Lac images a background sky level was subtracted from each image and elliptical isophotes were fit to the combined image of each object using the ellipse fitting routines of IRAF/STSDAS. This allowed us to determine that the unresolved point source components of each BL Lac are extremely well-centered in the surrounding nebulosity. Comparison of image centroids of the residual light in the point source function subtracted images shows that the limits on offsets between the total light (point source plus nebulosity) and the underlying nebulosities alone are  $\delta r < 0''.01$  for MS 1221.8+2452,  $\delta r < 0''.03$  for MS 1407.9+5954, and  $\delta r < 0''.01$  for MS 2143.4+0704. These results are consistent with the BL Lacs being perfectly centered in each of these cases.

We constructed azimuthally averaged semi-major axis radial profiles for each object and these are shown in Figure 1. To aid comparison of the profiles in Figure 1, we have

normalized the central intensity of the unsaturated point sources at a radius of zero. There is abundant excess extended light for each of the BL Lac objects when compared to the reference PSF profile seen in Figure 1. The radii to which the radial profiles are plotted in Figure 1 were determined by the point where the signal in the averaged surface brightness becomes comparable with instrumental read noise in the PC detector.

In Figures 2–4 we show for each of the BL Lacs the combined WFPC-2 PC image. In each figure the target object is in the approximate center. Objects with measured fluxes are labeled, and the aperture magnitudes and extents (resolved or point source) are listed in Tables 1–3. A large aperture of 150 pixels ( $6''.9$ ) is used for the host galaxy and host+PSF measurements quoted in the tables. Apertures with smaller radii of 6–20 pixels were used for measuring fainter objects in the field. The fields were well flattened, and although a small change in the DC sky level affects the integrated surface brightness and derived scale radius significantly, the aperture magnitudes are stable to much better than 0.1 mags over a large range of aperture radii.

Instrumental F814W magnitudes were converted to Kron-Cousins  $I$  pass-band using the formulas of Whitmore (1996). No reddening correction was applied. Uncertainties for the separate measurements of the host galaxy and the point source brightnesses are approximately 0.1 mag due to systematics in the PSF subtraction. The uncertainty in the measurement of the combined host+PSF brightness of each object is much smaller. The  $5\sigma$  limit on detection for faint point source objects is approximately  $I = 24.5$  in each of the three fields. As in Figure 1, it is clear in these images that the unresolved point source components of each BL Lac are surrounded by a resolved nebulosity.

An appropriately scaled model of the WFPC-2 instrumental PSF was subtracted from each BL Lac+underlying host (Yanny *et al.* 1997). Determining the appropriate scaling for the PSF is difficult for these well-centered objects, and there remains some uncertainty in the subtraction. Our normalizations were obtained by examining both the one dimensional radial profiles and the two dimensional residuals for a variety of PSF scalings. Figures 5, 6 and 7 show averaged semi-major axis plots of the profile of the PSF+host galaxy, host galaxy alone, and scaled PSF alone for the three objects we studied for this paper. Note that in each case, a De Vaucouleurs profile is a much better fit at small radii than an exponential disk (which would be expected if the host objects were spiral galaxies), and the extent to which a De Vaucouleurs profile is a better fit highlights the effectiveness of the resolving power of *HST* over ground-based observations. We use this evidence in §3 as part of the support for identifying all three host galaxies as elliptical galaxies.

As a check on the accuracy of the model PSF (Krist 1996) which we used for subtracting the contribution of the unresolved point source to the image of each BL Lac, several stellar

objects in the field were also fit and subtracted. We note that their radial profiles agree well with that of the model PSF out to a radius where their signal-to-noise ratio becomes low. To demonstrate the extent to which the host galaxy (underlying nebulosity) is present in all three cases, we present in Figure 8 an image of a field star in the MS 1407.9+5954 field, from which a model PSF has been subtracted. The BL Lac in Figure 8 has also had a scaled PSF subtracted from its image. The residual only contains the underlying nebulosity, and should be compared to the image in Figure 3. The inset in Figure 8 shows MS 1221.8+2452 after twice the correctly scaled PSF has been subtracted in order to show that a mis-scaled PSF subtraction when extended light is present does not remove light far from the core. The residual ring is clear evidence for an underlying host. No stellar object such as star D in Fig 8, shows a similar residual.

In Figure 9 we show contour maps, each  $4''.6 \times 4''.6$ , centered on the three BL Lacs with the same orientations as shown in Figures 2–4. The upper panels show the BL Lac+host galaxy before subtraction of the scaled PSF, and the lower panel shows the residual underlying host after a scaled PSF has been subtracted. The contours are geometrically spaced by factors of two in flux density, except for the outer 3 contours which are linearly spaced in flux density. We note that the contours for MS 2143.4+0704 appear boxy, further supporting its interpretation as a large elliptical host.

### 2.3. Notes on Individual Objects

In this section we present additional details about our measurements of the host galaxies of MS 1221.8+2452, MS 1407.9+5954, and MS 2143.4+0704 and compare our measured host galaxy properties to some of the existing observations of each object. We also make additional notes specific to the individual object fields. Observed quantities for field objects are listed in Tables 1–3. Physical properties of the host galaxies were calculated assuming  $H_0 = 50 \text{ km s}^{-1} \text{ Mpc}^{-1}$  and  $q_0 = 0$ , and are summarized in Table 4.

MS 1221.8+2452 ( $z = 0.218$ ) has a circular (ellipticity  $1 - b/a = 0.03 \pm 0.03$ ) host galaxy that is well fit by a De Vaucouleurs profile with a scale length of  $0''.68$  (3.2 kpc) and  $I_{KC} = 17.41$ . We measure an  $I_{KC}$  surface brightness (SB) at one scale length of  $\mu_I = 20.0 \text{ mag arcsec}^{-2}$ . For the unresolved point source component of the BL Lac we measured  $I_{KC} = 18.06$ . This object was successfully resolved by WSY during their CFHT imaging survey of BL Lacs. They observed MS 1221.8+2452 to contain a point source with Gunn r  $> 21.2$ . They determined the host galaxy had a brightness in the Gunn r pass-band of  $r=18.65$  with a surface brightness at one scale length of Gunn r  $\mu = 20.82 \text{ mag arcsec}^{-2}$ . WSY measured a scale length of  $0''.6$  (2.6 kpc).

MS 1407.9+5954 ( $z = 0.495$ ) was previously reported by WSY to have an elliptical host galaxy containing the point source BL Lac. We measure a host with an ellipticity of  $1 - b/a = 0.16 \pm 0.03$  at P.A.  $17^\circ$ , a De Vaucouleurs scale length of  $1''.52$  (12.2 kpc), and  $I_{KC} = 18.53$ . The SB( $I$ ) at one  $r_e$  is  $\mu_I = 22.3$  mag arcsec $^{-2}$ . For the BL Lac itself, we measure  $I_{KC} = 18.93$ . WSY determined a host galaxy brightness in the Gunn r pass-band of  $r = 19.37$ , with a surface brightness at 1 scale length of Gunn r  $\mu = 23.4$  mag arcsec $^{-2}$  and a scale length of  $1''.4$  (10 kpc). At the time WSY observed it, the central point source had Gunn  $r > 20.1$ .

MS 2143.4+0704 ( $z = 0.237$ ) has a host galaxy with an ellipticity  $1 - b/a = 0.20 \pm 0.02$  at P.A.  $64^\circ$ , a De Vaucouleurs scale length of  $1''.79$  (9.0 kpc) and  $I_{KC} = 17.13$ . The SB( $I$ ) at  $1 r_e$  is  $\mu_I = 21.3$  mag arcsec $^{-2}$ . For the point source, we measure  $I_{KC} = 18.58$ . Object L, near the BL Lac is very elongated, and is a candidate for a lensed arc. This BL Lac also has close companions D, F, and K within a few arcseconds. WSY quote Gunn  $r = 17.89$  for the large host object, with a SB of  $\mu = 22.95$  at one scale radius of  $2''.4$  (=12 kpc). The point source had a brightness of Gunn  $r = 22.2$  (WSY).

Given the different pass-bands and the variability of the BL Lacs, our measurements for the brightnesses and scale lengths of the host objects agree well with ground based measurements. Our uncertainties for the brightnesses of the host galaxies are estimated to be 0.1 mag (10%), dominated by systematics in the subtraction of the point source. To derive quantitative surface brightnesses and effective radii ( $r_e$ ) measurements, elliptical isophotes were fit to the image of each host galaxy and our tabulated results correspond to the values along the semi-major axis. Any deviation from a De Vaucouleurs profile in the underlying host galaxy (such as the boxy isophotes seen in MS 2143.4+0704) will result in a magnitude reconstructed from the surface brightness and scale radius which systematically differs from the fixed aperture magnitude measured for that object. Estimated uncertainties on these quantities are 0.2 mag on the surface brightnesses and 10% on the scale radii.

The WFPC-2 on *HST* provides some of the most accurate measurements to date of the nebulosity surrounding BL Lac sources because of the high dynamic range and spatial resolution provided in PC images. These properties allow the separation of PSFs from extended light at radii as small as  $\sim 0''.2$ .

### 3. Discussion

### 3.1. The Host Galaxies are Luminous Elliptical Galaxies

Our *HST* WFPC-2 observations of three X-ray selected BL Lacs confirm previous observations of these objects (*e.g.* WSY) that indicated that these BL Lacs are located in luminous elliptical host galaxies. The evidence supporting this conclusion includes the following:

1. The unresolved point source component of each BL Lac is extremely well-centered in the surrounding nebulosity or host galaxy light (see section 2.2), consistent with the point source being physically associated or “in” the nebulosity rather than a background source being lensed by a foreground galaxy. In this latter scenario some decentering would be expected (see WSY for discussion and references therein).
2. The available morphological evidence for each of the host galaxies strongly supports the classification of these objects as elliptical galaxies. Both the one dimensional (De Vaucouleurs profile fitting) and two dimensional appearance of the host galaxies (see Figures 2–4 and Figure 9) are more consistent with these objects being elliptical galaxies than spirals. The least squares fits to the residual light after subtraction of a scaled point source show a much better fit by a De Vaucouleurs profile than by an exponential disk profile (see Figures 5–7). There is evidence for boxy isophotes in one of the host galaxies, a characteristic shared by many elliptical galaxies, while there are no signs in any of the host galaxies of “bars”, spiral arms, or other substructures that might be expected in a spiral host galaxy. The observed ellipticities and scale radii are also consistent with the properties of elliptical galaxies.
3. The detected host galaxies are luminous. In Table 4 we list the observed and derived absolute magnitudes for the three X-ray selected BL Lac objects in this paper as well as the two radio selected BL Lac objects imaged with *HST* by Falomo *et al.* (1997) and the radio and X-ray selected BL Lac OJ 287 imaged by Yanny *et al.* (1997). A K-correction has been applied to each absolute magnitude based on the catalogued redshift of the BL Lac, our assumed cosmology, and the typical rest frame colors of ellipticals assumed by Falomo *et al.* (1997) when they made similar calculations to derive the absolute magnitudes of their detected host galaxies ( $V - I = 1.3$ ,  $B - V = 0.96$ , and  $V - R = 0.61$ ). No correction for the effects of spectral evolution have been made (as was done by WSY). If we were to include the effects of evolution in order to derive what the absolute magnitudes of these host galaxies would be if they were evolved to the current epoch, then this might result in a change of from 0.2 mag (for objects at  $z \approx 0.2$ ) to 0.6 mag (for objects at  $z \approx 0.5$ ) in the absolute magnitudes of the objects (see Poggianti 1997 for examples of the size of



the evolutionary corrections required for a given observed band and assumed intrinsic spectral energy distribution). While assuming normal elliptical colors for these host galaxies is probably not unreasonable, we have only obtained *F814W* pass-band images with *HST*. Comparing with the ground based measurements of WSY, the  $r - I_{\text{KC}}$  colors of the three objects are 1.2, 0.8 and 0.8 mags respectively. The derived host galaxy absolute magnitudes (*e.g.*  $-23.4 < M_V < -22.2$ ) are within the range of observed luminosities of brightest cluster galaxies (BCG), although perhaps not as bright as the brightest of BCG (the more luminous BCG have  $M_V \approx -23.6$ , Hoessel & Schneider 1985; Postman & Lauer 1995; see WSY and Hoessel *et al.* 1980 for distribution of BCG luminosities). If spectral evolution is significant, as seems likely, then since the comparison sample of BCG are typically at redshifts of 0.15, a significant evolution correction would only have to be applied to the results for MS 1407.9+5954. Before comparing the absolute magnitude of this object’s host galaxy to the distribution of BCG absolute magnitudes we should make fainter the absolute magnitude of MS 1407.9+5954 by 0.4 to 0.6 of a magnitude. As a result, MS 1407.9+5954 would be fainter than the brightest BCG, but still quite a luminous elliptical.

### 3.2. Comparison With Other AGN Host Galaxies

One of the main goals of studying the properties of the host galaxies of BL Lacs is to allow a comparison between the observed properties of the hosts of BL Lacs and the host galaxies of other AGN and candidate parent populations (*e.g.* comparing to the observed properties of the host galaxies and environments of Farnaroff-Riley I and II radio galaxies; *e.g.* Zirbel 1996ab, 1997). The largest optical survey of BL Lac host galaxy properties, ground or space based, is the survey of made by WSY. They imaged 50 BL Lacs with the Canada France Hawaii Telescope and resolved a host galaxy in over 90% of the objects. Based on radial profile fits to their images they classified at least 70% (possibly as high as 90%) of the detected host galaxies as ellipticals, with no more than 12% showing exponential disk or spiral type hosts.

Despite our small sample size and the resulting inability to draw new conclusions for the entire class of BL Lac objects, we can place the objects we observed “in context” by comparing the magnitudes of the hosts of the objects we observed to other well observed BL Lac or quasar host galaxies. For example, when our XSBLs are compared to a sample of Radio Selected BL Lacs studied by Falomo *et al.* (1997) at a comparable redshift, the XSBL host galaxies are found to be about one magnitude fainter than those of BL Lacs

selected by their radio emission, while still being quite luminous.

We can also compare our BL Lac host galaxies to those observed in the larger sample of luminous low redshift quasars that have been observed with WFPC-2, as the nuclear luminosity generating mechanisms may (or may not) be similar. Bahcall *et al.* (1997) have surveyed the hosts of 20 QSOs with *HST* resolution at redshifts  $\sim 0.2$ . The host galaxies of radio quiet QSOs are ellipticals in more than 60% of the cases and have  $\langle M_V \rangle = -22.2 \pm 0.6$  on average, about the same magnitude as those seen here for XSBL hosts at  $z=0.2$  (see Table 4).

### 3.3. Companion Objects

The field of the WFPC-2 PC CCD is  $36'' \times 36''$ . At redshift  $z = 0.2$ , the radius of the field corresponds to  $r < 90$  kpc. All objects within this radius of the three BL Lacs that are the focus of this paper were noted in the figures and in Tables 1, 2, and 3. Since redshifts of these objects are not known, one cannot tell for certain which objects are true companions to the BL Lacs, however, objects within a projected distance of a few arcseconds of the BL Lac and brighter than about  $I < 24$  are likely to be physically associated with the BL Lac. We note that based on the Hubble Deep Field galaxy counts (Williams *et al.* 1996), the number of galaxies expected with  $I_{814} < 23.5$  in a circular patch of radius  $17''$  is  $\sim 4$ .

The field of MS 1221.8+2452 has only three objects in the field other than the BL Lac+host, and none are within  $10''$ . This appears to be an isolated BL Lac.

In contrast, the field of MS 1407.9+5954 is relatively rich, with 20 objects in the field, all but two of them are non-stellar. MS 1407.9+5954 may be in a relatively rich group or cluster (see also Wurtz *et al.* 1993).

The field of MS 2143.4+0704 is intermediate between the other two in the number of objects in the field, with 12 non-stellar objects. It has, however, several very close neighbors which are likely to be physically associated with MS 2143.4+0704. The objects D and F are especially likely to be associated with the BL Lac. Object L is of interest because its elongation and alignment is reminiscent of gravitationally lensed objects seen in the field of massive clusters. A redshift of object L and further analysis are needed. We note that *HST* has provided images with similarly elongated objects that have proven to be spiral galaxies.

Our three randomly selected XSBLs show differing field environments. This demonstrates clearly, if not unexpectedly, that a sample of three objects is not large enough to draw any conclusions about the role that environment may play in the BL Lac

phenomenon. The richness of the environments of larger samples of BL Lac objects has been quantitatively studied using ground-based imaging data (*e.g.* Wurtz *et al.* 1997, including data on the three objects studied in this paper), but such studies still lack spectroscopic confirmation of the association with the BL Lacs of the apparent companion objects. Spectroscopic follow-up would be valuable not only to confirm group membership, but also to determine velocity dispersions for the groups.

#### 4. Summary

We have presented *HST* WFPC-2 *I*-band (F814W) images of three X-ray selected BL Lacs, measured the properties of the BL Lac host galaxies, and catalogued the companion objects in the fields of these BL Lac objects. From these data we have determined the following:

1. The host galaxies of the X-ray selected BL Lacs MS 1221.8+2452, MS 1407.9+5954, and MS 2143.4+0704 are luminous elliptical galaxies with absolute luminosities in the range  $-24.7 < M_I < -23.5$ ). These host galaxies appear typical of the BL Lac host galaxies that have been previously observed.
2. The three XSBLs observed in our program have a wide range in the apparent number of companion objects, but without spectra or color information to allow a more accurate determination of which objects are true companions of each BL Lac we are not able to further investigate whether or not the larger scale environments of these three objects are disparate nor are we able to compare their environments to those of other BL Lacs studied by others (*e.g.* Wurtz *et al.* 1997).
3. The absolute magnitudes of the BL Lac hosts near  $z=0.2$  have absolute magnitudes comparable to those of radio quiet QSO hosts seen in Bahcall *et al.* (1997). There is a suggestion that XSBL host galaxies might be fainter than RSBL hosts, but this needs to be tested with high quality imaging of larger and well defined samples.

The small sample of 6 objects that have been well imaged by *HST* (this paper; the two objects with detected host galaxies in Falomo *et al.* 1997; and OJ 287, Yanny *et al.* 1997) is not large enough to draw strong conclusions about “all” BL Lacs or differences in sub-groupings. Fortunately additional objects are being imaged and the total sample size will certainly grow. *HST* imaging offers the potential of undertaking studies of higher redshift objects that can be integrated into the larger data sets of images of low redshift BL Lacs.

We acknowledge useful discussions with A. Dey, R. Falomo, T. Lauer, S. Kent, R. Scarpa, and J. Stocke. We acknowledge support from NASA grant GO-5992.02-94A. B.Y. acknowledges support from the Fermi National Accelerator Laboratory. B.T.J. acknowledges support from the National Optical Astronomy Observatories, operated by the Associated Universities for Research in Astronomy, Inc., under cooperative agreement with the National Science Foundation.

## REFERENCES

- Abraham, R. G., Crawford, C. S. & McHardy, I. M. 1991, MNRAS, 252, 482
- Bahcall, J. N., Kirhakos, S., Saxe, D. H., & Schneider, D. P. 1997, Ap.J., 479, 642
- Blandford, R., & Rees, M. 1978 in Pittsburgh Conference on BL Lac Objects, ed. A. M. Wolfe (Pittsburgh: Univ. Pittsburgh Press), p. 328
- Disney, M. J., Boyce, P. J., Blades, J. C., Boksenberg, A., Crane, P., Deharveng, J. M., Macchetto, F., Mackay, C. D., Sparks, W. B., & Phillipps, S. 1995, Nature, 376, 150
- Falomo, R. 1996, MNRAS, 283, 241
- Falomo, R., Urry, C. M., Pesce, J. E., Scarpa, R., Biavalisco, M., & Treves, A. 1997, Ap.J., 476, 113
- Hoessel, J. G., Gunn, J. E., & Thuan, T. X. 1980, Ap.J. 241, 486
- Hoessel, J. G., & Schneider, D. P. 1985, A.J., 90, 1648
- Holtzman, J. A. *et al.* 1995, PASP, 107, 156
- Hooper, E., Impey, C., & Foltz, C. 1997, Ap.J., 480, L95
- Impey, C., & Neugebauer, G. 1988 A.J. 95, 307
- Jannuzi, B. T. 1990, Ph.D. thesis, Univ. of Arizona
- Jannuzi, B. T., Smith, P. S., & Elston, R. 1993, Ap.J.S., 85, 265
- Jannuzi, B. T., Smith, P. S., & Elston, R. 1994, Ap.J., 428, 130
- Krist, J. 1996, STSCI Tiny Tim Software, personal communication
- McLeod, K. K., & Rieke, G. H. 1995, Ap.J., 454, 77
- Morris, S., Stocke, J. T., Gioia, I. M., Schild, R. E., Wolter, A., Maccacaro, T., & Della Ceca, R. 1991, Ap.J., 380, 49
- Miller, J. S., French, H. B., & Hawley, S. A. 1978, Ap.J., 219, L85
- Oke, J. B., & Gunn, J. E. 1974, Ap.J., 189, L50

- Pesce, J. E., Falomo, R., & Treves, A. 1994, *A.J.*, 107, 494
- Pesce, J. E., Falomo, R., & Treves, A. 1995, *A.J.*, 110, 1554
- Poggianti, B. M. 1997, *A.&A.S.*, 122, 399
- Postman, M., & Lauer, T. R. 1995, *Ap.J.*, 440, 28
- Smith, P. S., Jannuzi, B. T., & Elston, R. 1991, *Ap.J.S.*, 77, 67
- Stocke, J., Liebert, J., Schmidt, G., Gioia, I. M., Maccacaro, T., Schild, R. E, Maccagni, D., & Arp H. C. 1985, *Ap.J.*, 298, 619
- Thuan, T. X., Oke, J. B., Gunn, J. E. 1975, *Ap.J.*, 201, 45
- Ulrich, M.-H., Kinman, T. D., Lynds, C. R., Rieke, G. H., & Ekers, R. D. 1975, *Ap.J.*, 198, 261
- Ulrich, M.-H. 1989, in *BL Lac Objects*, ed. L. Maraschi, T. Maccacaro, & M.-H. Ulrich (Berlin: Springer), 45
- Urry, C. M., & Padovani, P. 1995, *PASP*, 107, 803
- Wagner, S. J., & Witzel, A. 1995, *ARAA*, 33, 163
- Whitmore, B. 1996, *WFPC-2 Photometry Cookbook*, personal communication
- Williams, R. E. *et al.* 1996, *A.J.*, 112, 1335
- Wurtz, R., Ellingson, E., Stocke, J. T., & Yee, H. K. C. 1993, *A.J.*, 106, 869
- Wurtz, R., Stocke, J. T., & Yee, H. K. C. 1996, *Ap.J.S.*, 103, 109 (WSY)
- Wurtz, R., Stocke, J. T., & Ellingson, E., & Yee, H. K. C. 1997, *Ap.J.*, 480, 547
- Yanny, B., Guhathakurta, P., Schneider, D. P., & Bahcall, J. N. 1994, *Ap.J.L.*, 435, L59
- Yanny, B., Jannuzi, B. T. & Impey, C. 1997, *ApJL* in press
- Zirbel, E. L. 1996a, *Ap.J.*, 473, 144
- Zirbel, E. L. 1996b, *Ap.J.*, 473, 713
- Zirbel, E. L. 1997, *Ap.J.*, 476, 489

### FIGURE CAPTIONS

Fig. 1.— Averaged semi-major axis profiles of three BL Lac objects plus a bright model field star to show the PSF. All three of the BL Lacs clearly show extensive extended light in excess of that expected from an isolated point source.

Fig. 2.— Image obtained with the WFPC-2 PC of the MS 1221.8+2452 field. The BL Lac and host is in the center of the image. No subtraction has been performed. Measurements for labeled objects are listed in Table 1.

Fig. 3.— Image obtained with the WFPC-2 PC of the MS 1407.9+5954 field. The BL Lac and host is in the center of the image. No subtraction has been performed. Measurements for labeled objects are listed in Table 2. Note the rich field.

Fig. 4.— Image obtained with the WFPC-2 PC of the MS 2143.4+0704 field. The BL Lac and host is in the center of the image. No PSF subtraction has been performed. Measurements for labeled objects are listed in Table 3. Note the close companions D and L. L is very elongated. The apparent “ejecta” from the SE of the object is a diffraction spike produced by the central point source.

Fig. 5.— Elliptical isophote fits to the image of MS 1221.8+2452. The upper solid line shows the radial profile (elliptical semi-major axis) of the sky-subtracted data. The lower solid line is a *HST* stellar point spread function scaled to match the point source component of the BL Lac image. The asterisks mark the underlying host galaxy light once the scaled point source has been centered and subtracted from the image. The filled circles represent the best least chi-squared fit for a De Vaucouleurs profile to the host galaxy light for radii between  $0''.15$  and  $1''.5$ . The open circles represent the best fit exponential disk profile to the host galaxy light. The small error ticks at  $1''.6$  and  $2''.1$  show read noise induced errors in the surface brightness measurements.

Fig. 6.— Same as Fig. 5, but for MS 1407.9+5954.

Fig. 7.— Same as Fig. 5, but for MS 2143.4+0704.

Fig. 8.— In this image are displayed the results of subtracting a scaled PSF from several objects in our images. In the main image, the Galactic field star labeled D, has had a PSF scaled and subtracted from it. Note the complete lack of any diffuse emission beyond the core of the residual. This is the expected result for all point source objects. In contrast, after subtraction of a scaled PSF from MS 1407.9+5954 (shown in the center of the image), there is considerable residual extended emission from the elliptical host galaxy. In the inset, a PSF of twice the fitted value was intentionally over-subtracted from MS 1221.8+2452 to

show the extended emission in contrast to the lack of emission surrounding the field star D in the main field.

Fig. 9.— Contour plots of the images of the central  $4''.6 \times 4''.6$  boxes of each of the three BL Lac objects before (upper panels) and after (lower panels) scaled PSF subtraction. Each of the point sources is well-centered on its host galaxy. The isophotes for object MS 2143.4+0704 appear boxy, additional evidence that this host galaxy is an elliptical. The ring of circles seen in MS 1221.8+2452 after PSF subtraction are due to slight changes in the *HST* diffraction level optics between the BL Lac and the model PSF.

Table 1: Objects in the Field of MS 1221.8+2452

| ID             | $\Delta\text{RA}(\prime\prime)$ | $\Delta\text{DEC}(\prime\prime)$ | $I_{KC}$ mag | FWHM( $\prime\prime$ ) <sup>a</sup> |
|----------------|---------------------------------|----------------------------------|--------------|-------------------------------------|
| MS 1221.8+2452 | 0.00                            | 0.00                             | 16.94        | ext                                 |
| HOST           | 0.00                            | 0.00                             | 17.41        | 0.68 <sup>b</sup>                   |
| POINT SOURCE   | 0.00                            | 0.00                             | 18.06        | pt                                  |
| A              | −8.12                           | −12.41                           | 21.24        | 0.14                                |
| B              | −10.52                          | 9.10                             | 21.41        | 0.14                                |
| C              | 13.60                           | −2.54                            | 22.27        | ext                                 |

<sup>a</sup>The label “ext” indicates the object is significantly extended, while “pt” indicates a point source.

<sup>b</sup>For the host galaxy (HOST), FWHM is replaced by the elliptical scale radius  $r_e$ .



Table 2: Objects in the Field of MS 1407.9+5954

| ID             | $\Delta\text{RA}(\prime\prime)$ | $\Delta\text{DEC}(\prime\prime)$ | $I_{KC}$ mag | FWHM( $\prime\prime$ ) <sup>a</sup> |
|----------------|---------------------------------|----------------------------------|--------------|-------------------------------------|
| MS 1407.9+5954 | −0.00                           | −0.01                            | 17.96        | ext                                 |
| HOST           | −0.00                           | −0.01                            | 18.53        | 1.52 <sup>b</sup>                   |
| POINT SOURCE   | 0.29                            | 0.16                             | 18.93        | pt                                  |
| A              | −8.30                           | −9.02                            | 17.81        | ext                                 |
| B              | −7.40                           | −5.74                            | 20.68        | 0.11                                |
| C              | 0.18                            | −11.15                           | 20.99        | 0.09                                |
| D              | 10.58                           | −10.98                           | 18.60        | pt                                  |
| E              | 5.22                            | 2.91                             | 21.18        | 0.12                                |
| F              | −12.78                          | 0.99                             | 21.69        | 0.17                                |
| G              | 11.21                           | −7.83                            | 21.51        | 0.09                                |
| H              | −14.19                          | 6.31                             | 22.69        | 0.11                                |
| I              | −20.91                          | −3.37                            | 22.13        | 0.1                                 |
| J              | −22.39                          | −0.84                            | 21.47        | ext                                 |
| K              | 8.45                            | 9.52                             | 22.78        | 0.27                                |
| L              | 9.91                            | 6.93                             | 23.69        | 0.11                                |
| M              | 16.00                           | 1.78                             | 23.35        | 0.15                                |
| N              | 2.95                            | −16.39                           | 23.52        | pt                                  |
| O              | −6.93                           | −1.94                            | 24.30        | 0.09                                |
| P              | −3.21                           | −5.32                            | 24.39        | 0.34                                |
| Q              | −5.16                           | 2.65                             | 24.91        | ext                                 |
| R              | −10.46                          | 4.60                             | 23.85        | 0.17                                |
| S              | 3.02                            | 5.33                             | 24.70        | 0.13                                |
| T              | 5.44                            | −13.39                           | 24.99        | ext                                 |

<sup>a</sup>The label “ext” indicates the object is significantly extended, while “pt” indicates a point source.

<sup>b</sup>For the host galaxy (HOST), FWHM is replaced by the elliptical scale radius  $r_e$ .

Table 3: Objects in the Field of MS 2143.4+0704

| ID             | $\Delta\text{RA}(\prime\prime)$ | $\Delta\text{DEC}(\prime\prime)$ | $I_{KC}$ mag | FWHM( $\prime\prime$ ) <sup>a</sup> |
|----------------|---------------------------------|----------------------------------|--------------|-------------------------------------|
| MS 2143.4+0704 | 0.00                            | −0.00                            | 16.88        | ext                                 |
| HOST           | 0.00                            | −0.01                            | 17.13        | 1.79 <sup>b</sup>                   |
| POINT SOURCE   | 0.00                            | −0.01                            | 18.58        | pt                                  |
| A              | −6.79                           | −9.87                            | 18.88        | pt                                  |
| B              | −15.87                          | −3.29                            | 20.10        | 0.02                                |
| C              | −15.92                          | 9.48                             | 22.09        | ext                                 |
| D              | −1.31                           | 0.99                             | 23.60        | 0.18                                |
| E              | −2.38                           | 6.34                             | 23.14        | 0.09                                |
| F              | −3.97                           | 1.64                             | 23.37        | 0.03                                |
| G              | −12.95                          | 13.56                            | 23.33        | 0.09                                |
| H              | −13.67                          | 9.21                             | 24.19        | 0.05                                |
| I              | −5.28                           | 14.66                            | 23.71        | ext                                 |
| J              | 1.35                            | 6.17                             | 24.57        | pt                                  |
| K              | −0.62                           | 3.28                             | 25.63        | ext                                 |
| L              | −0.47                           | −2.56                            | 24.97        | ext                                 |
| M              | −18.75                          | 13.62                            | 24.48        | ext                                 |
| N              | 4.72                            | −11.56                           | 23.65        | ext                                 |
| O              | 2.40                            | −7.75                            | 24.87        | ext                                 |

<sup>a</sup>The label “ext” indicates the object is significantly extended, while “pt” indicates a point source.

<sup>b</sup>For the host galaxy (HOST), FWHM is replaced by the elliptical scale radius  $r_e$ .

Table 4: Magnitudes of Selected BL Lacertae Object Host Galaxies

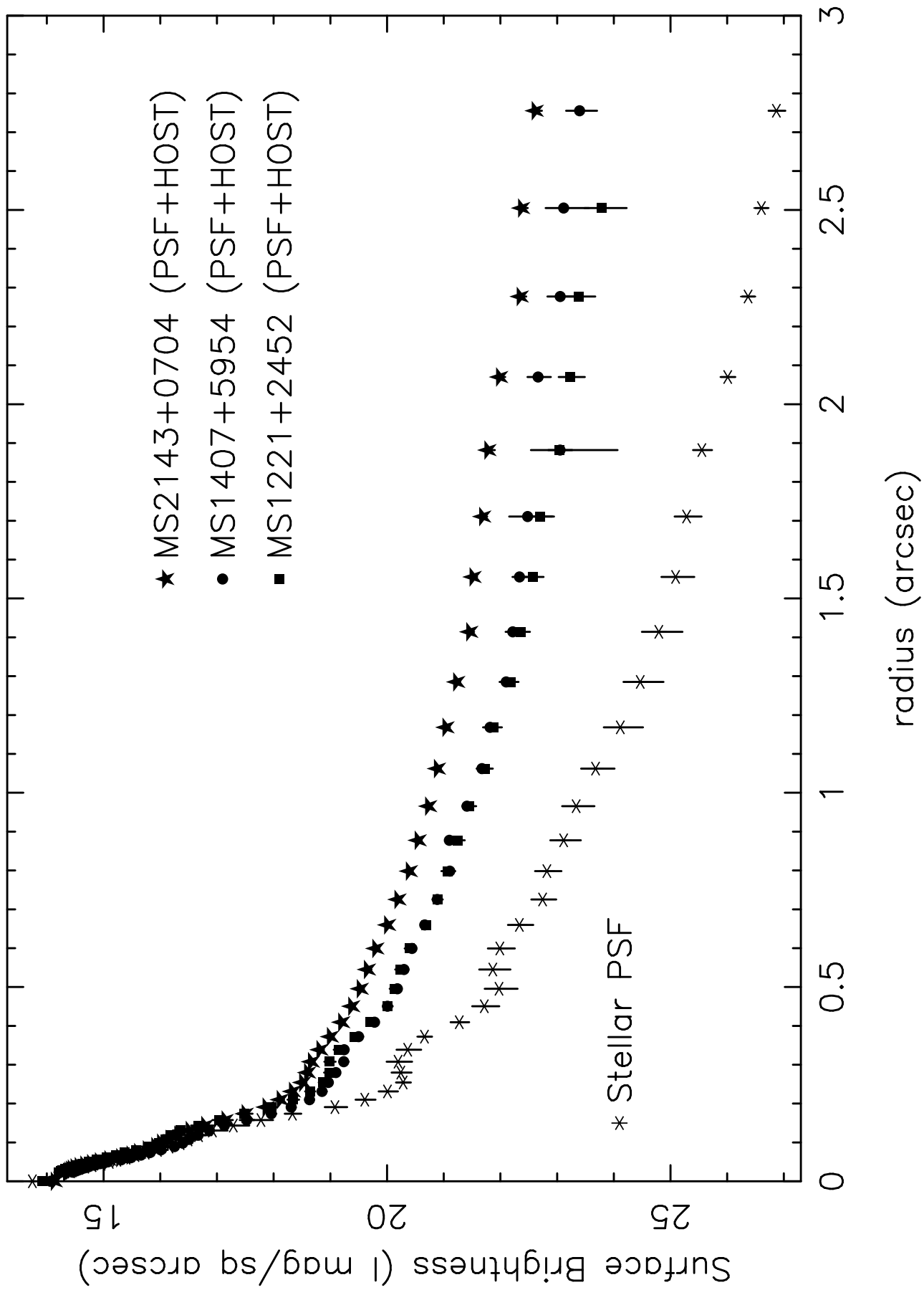
| Name                  | $I$   | redshift | $k_{\text{corr}}$ | m-M   | $M_I^{\text{a}}$ | $M_R^{\text{b}}$ | $M_V^{\text{b}}$ | $r_e$ (kpc) <sup>a</sup> |
|-----------------------|-------|----------|-------------------|-------|------------------|------------------|------------------|--------------------------|
| 1823+568 <sup>c</sup> | 18.3  | 0.664    | 0.54              | 43.72 | -26.0            | -25.3            | -24.7            | 6.5                      |
| 2254+074 <sup>c</sup> | 15.9  | 0.19     | 0.11              | 40.49 | -24.7            | -24.0            | -23.4            | 15.0                     |
| MS 1221.8+2452        | 17.41 | 0.218    | 0.13              | 40.81 | -23.5            | -22.8            | -22.2            | 3.2                      |
| MS 1407.9+5954        | 18.53 | 0.495    | 0.37              | 42.84 | -24.7            | -24.0            | -23.4            | 12.2                     |
| MS 2143.4+0704        | 17.13 | 0.237    | 0.14              | 41.01 | -24.0            | -23.3            | -22.7            | 9.0                      |
| OJ 287 <sup>d</sup>   | 18.3  | 0.306    | 0.19              | 41.65 | -23.5            | -22.8            | -22.2            | –                        |

<sup>a</sup> $H_0 = 50 \text{ km s}^{-1} \text{ Mpc}^{-1}$ ,  $q_0 = 0$ ,  $M_I = I - (m-M) - K\text{-corr}$

<sup>b</sup> $V - I = 1.3$ ,  $V - R = 0.6$ , are assumed, as in Falomo *et al.* (1997)

<sup>c</sup>The radio selected BL Lac host data from Falomo *et al.* (1997).

<sup>d</sup>OJ 287 BL Lac host data from Yanny *et al.* (1997).



This figure "fig2.jpg" is available in "jpg" format from:

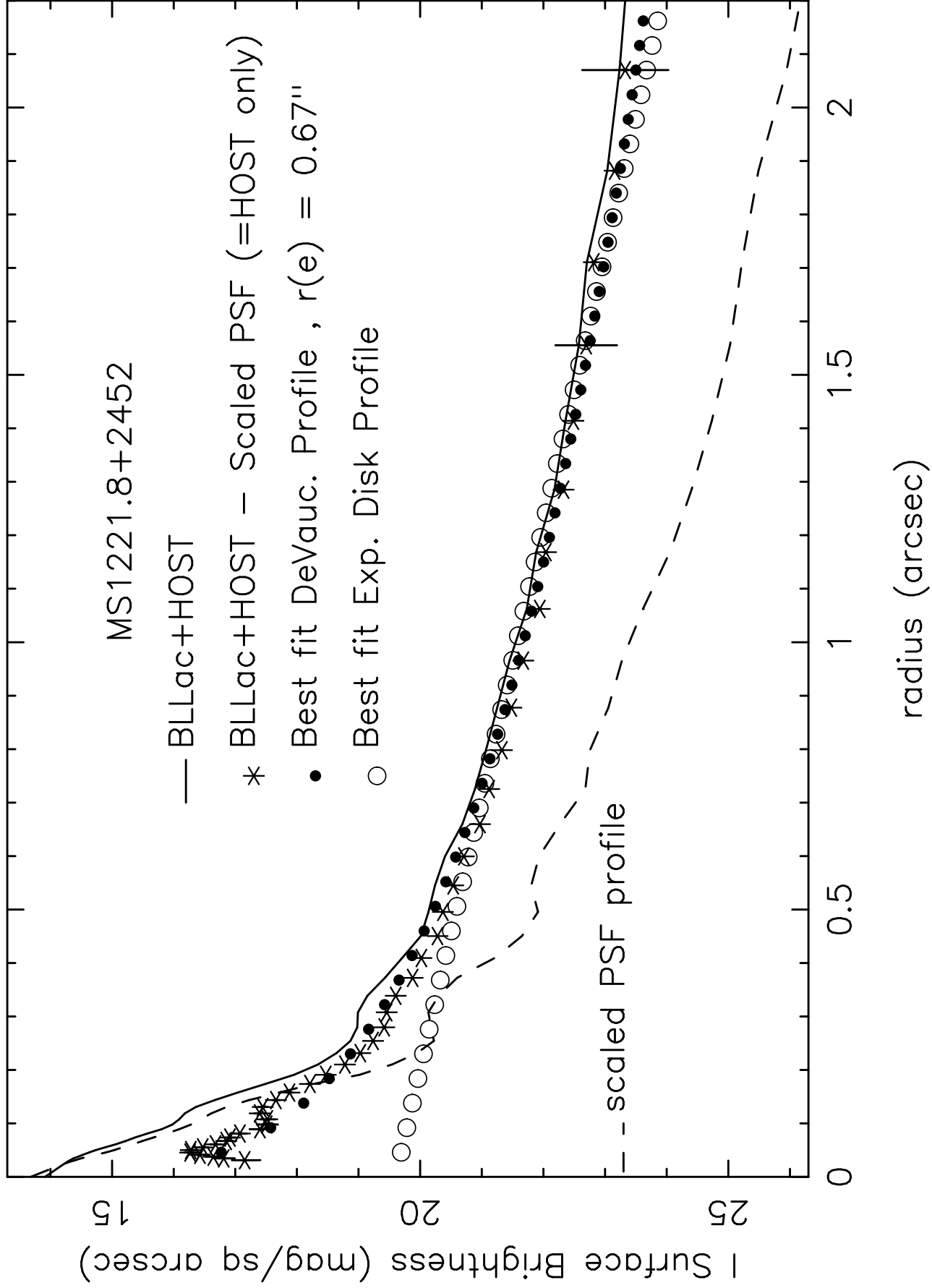
<http://arxiv.org/ps/astro-ph/9706028v2>

This figure "fig3.jpg" is available in "jpg" format from:

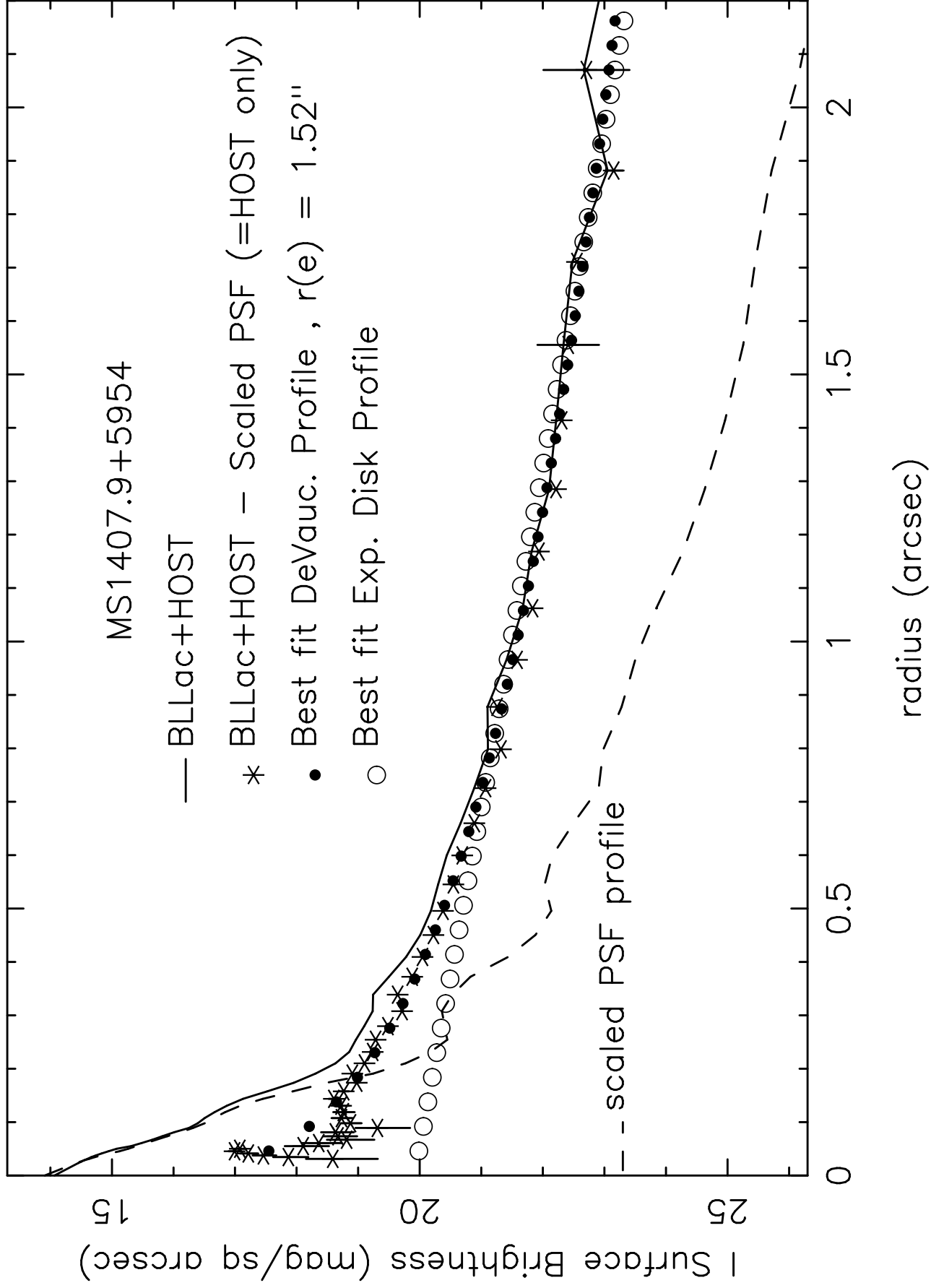
<http://arxiv.org/ps/astro-ph/9706028v2>

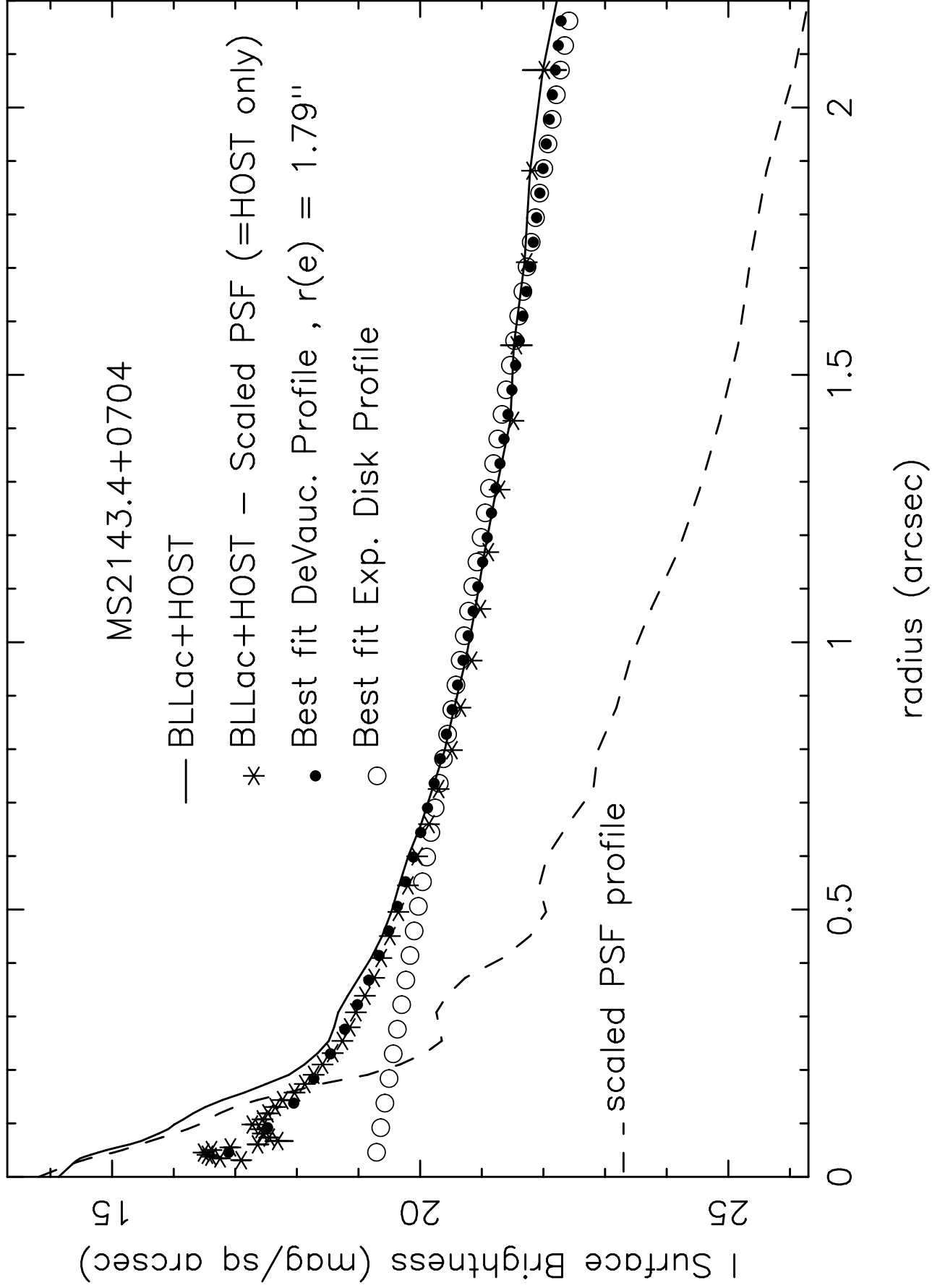
This figure "fig4.jpg" is available in "jpg" format from:

<http://arxiv.org/ps/astro-ph/9706028v2>





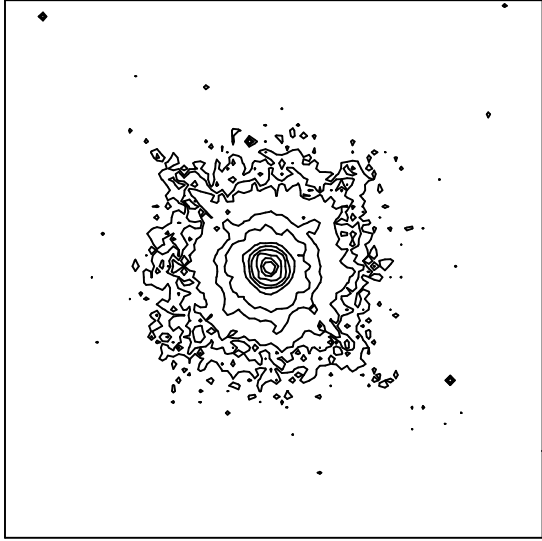




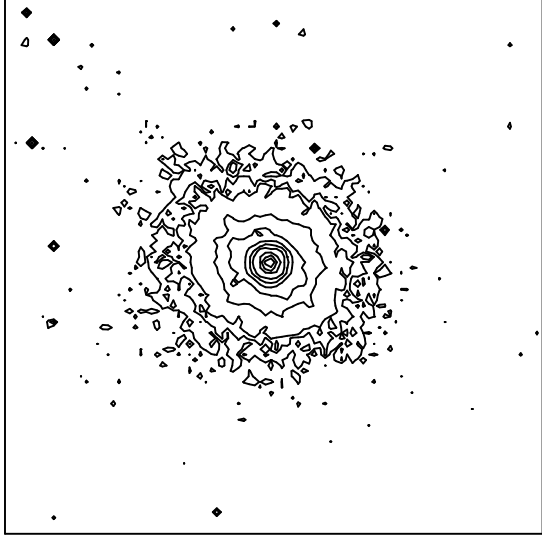
This figure "fig8.jpg" is available in "jpg" format from:

<http://arxiv.org/ps/astro-ph/9706028v2>

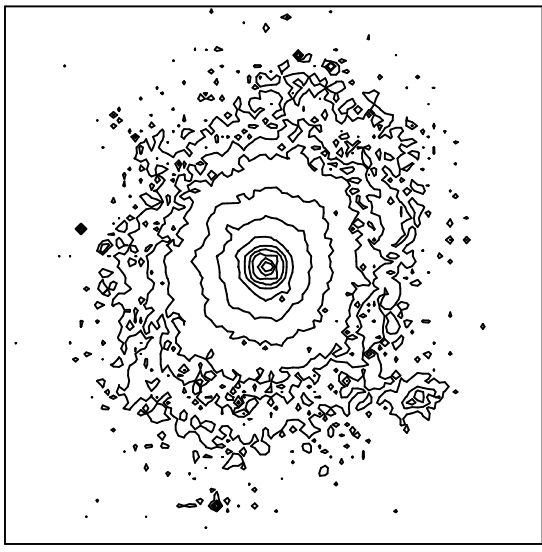
MS1221.8+2452



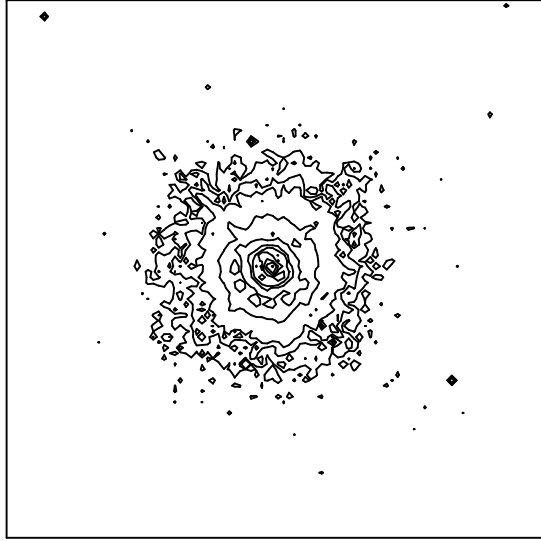
MS1407.9+5954



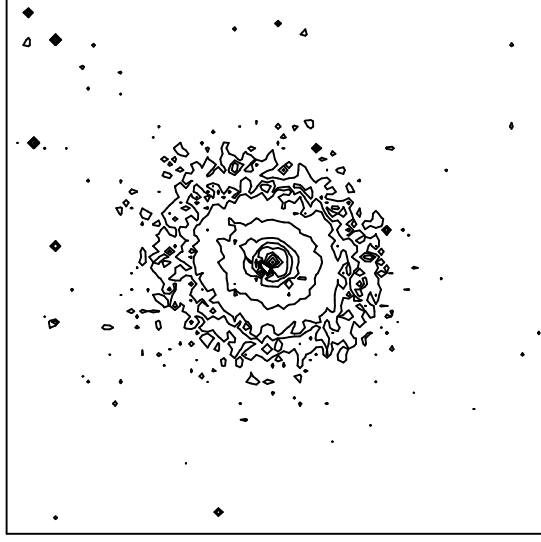
MS2143.4+0704



MS1221.8+2452 - PSF



MS1407.9+5954 - PSF



MS2143.4+0704 - PSF

